



HAL
open science

Adenomyosis is associated with specific proton nuclear magnetic resonance ($^1\text{H-NMR}$) serum metabolic profiles

Mathilde Bourdon, Pietro Santulli, Fatiha Kateb, Khaled Pocate-Cheriet, Frederic Batteux, Chloé Maignien, Sandrine Chouzenoux, Corinne Bordonne, Louis Marcellin, Gildas Bertho, et al.

► To cite this version:

Mathilde Bourdon, Pietro Santulli, Fatiha Kateb, Khaled Pocate-Cheriet, Frederic Batteux, et al.. Adenomyosis is associated with specific proton nuclear magnetic resonance ($^1\text{H-NMR}$) serum metabolic profiles. *Fertility and Sterility*, 2021, 116 (1), pp.243-254. 10.1016/j.fertnstert.2021.02.031 . hal-03684698

HAL Id: hal-03684698

<https://u-paris.hal.science/hal-03684698>

Submitted on 2 Aug 2023

HAL is a multi-disciplinary open access archive for the deposit and dissemination of scientific research documents, whether they are published or not. The documents may come from teaching and research institutions in France or abroad, or from public or private research centers.

L'archive ouverte pluridisciplinaire **HAL**, est destinée au dépôt et à la diffusion de documents scientifiques de niveau recherche, publiés ou non, émanant des établissements d'enseignement et de recherche français ou étrangers, des laboratoires publics ou privés.



Distributed under a Creative Commons Attribution - NonCommercial 4.0 International License

TITLE: Adenomyosis is associated with specific proton nuclear magnetic resonance ($^1\text{H-NMR}$) serum metabolic profiles

Running title: $^1\text{H-NMR}$ serum metabolic profiles in adenomyosis

Bourdon Mathilde, MD ^{1,2,3,4*+}
Santulli Pietro, MD PhD ^{1,2,3,4+}
Kateb Fatiha, PhD ^{5,6+}
Pocate-Cheriet Khaled, MD ^{1,2,4,7}
Batteux Frederic, MD PhD ^{1,2,4,}
Maignien Chloé MD ^{1,2,3}
Chouzenoux Sandrine ⁴
Bordonne Corinne, MD ^{2,9}
Marcellin Louis, MD PhD ^{1,2,3,4}
Bertho, Gildas, PhD ^{5,6†*}
Chapron Charles, MD ^{1,2,3,4 †}

¹ *Université de Paris, Faculty of Medicine, Paris, France*

² *Assistance Publique–Hôpitaux de Paris (AP–HP), Hôpital universitaire Paris Centre (HUPC), Paris, France*

³ *Department of Gynaecology Obstetrics II and Reproductive Medicine, Cochin University Hospital Center (UHC), Paris, France*

⁴ *Department 3I “Infection, Immunité et inflammation”, Cochin Institute, INSERM U1016, Paris, France*

⁵ *Université de Paris, Faculty of Sciences, Campus Saint-Germain-des-Prés, Paris, France*

⁶ *Laboratory of Pharmacological and Toxicological Chemistry and Biochemistry, UMR 8601-CNRS, Paris, France*

⁷ *Department of Histology–Embryology and Reproductive Biology, Cochin University Hospital Center (UHC), Paris, France*

⁸ *Department of Immunology, Cochin University Hospital Center (UHC), Paris, France*

⁹ *Department of Radiology, Hôtel-Dieu University Hospital Center (UHC), Paris, France*

+ *Mathilde Bourdon, Pietro Santulli, and Fatiha Kateb should be considered similar in author order.*

† *Gildas Bertho and Charles Chapron should be considered similar in author order.*

CORRESPONDING AUTHOR:

Dr. BERTHO Gildas, PhD

Laboratoire de Chimie et Biochimie Pharmacologiques et Toxicologiques, UMR 8601-CNRS

Université de Paris, Campus Saint-Germain-des-Prés

45 rue des Saint-Pères 75006 Paris, France

Phone: +33-1-42-86-21-80 - Email: gildas.bertho@u-paris.fr

Capsule

Adenomyosis serum samples have distinct and adenomyosis phenotype specific $^1\text{H-NMR}$ -based serum metabolic profiles. The metabolites with altered levels are involved in immunity, cell proliferation, and cell migration.

ABSTRACT

Objective: To determine whether the adenomyosis phenotype affects the $^1\text{H-NMR}$ -based serum metabolic profile of patients.

Design: A cohort study

Setting: A university hospital-based research center

Patients/Animals: 77 patients who underwent laparoscopy for a benign gynecological condition.

Interventions: Pelvic magnetic resonance imaging and collection of a venous peripheral blood sample were performed during the preoperative work-up. The women were allocated to the adenomyosis group ($n=32$), or to the control group ($n=45$). The adenomyosis group was further subdivided into two groups: diffuse adenomyosis of the inner myometrium ($n=14$) and focal adenomyosis of the outer myometrium (FAOM) ($n=18$). Other adenomyosis phenotypes were excluded.

Main outcomes measures: Metabolomic profiling based on $^1\text{H-NMR}$ spectroscopy in combination with statistical approaches.

Results: The serum metabolic profiles of the patients with adenomyosis indicated lower concentrations of 3-hydroxybutyrate ($p=0.02$), glutamate ($p=0.02$), and serine ($p=0.04$) compared to the controls. Conversely, the concentrations of proline ($p=0.01$), choline ($p=0.02$), citrate ($p=0.05$), 2-hydroxybutyrate ($p=0.04$), and creatinine ($p<0.01$) were higher in the adenomyosis group. The FAOM and the diffuse adenomyosis phenotypes also each exhibited a specific metabolic profile.

Conclusion: Serum metabolic changes were detected in women with features of adenomyosis compared to their disease-free counterparts, and a number of specific metabolic pathways appear to be engaged according to the adenomyosis phenotype. The metabolites with altered levels are particularly involved in immune activation as well as cell proliferation and cell migration. Nevertheless, this study did find evidence of a correlation between metabolite levels and symptoms thought to be related to adenomyosis. Further studies are required to determine the clinical significance of these differences in metabolic profiles.

KEYWORDS: Adenomyosis; Metabolomics; Serum; $^1\text{H-NMR}$; MRI

INTRODUCTION

Adenomyosis is a benign uterine disorder historically characterized by the presence of endometrial glands and stroma within the myometrium (1). Although histological analysis is the gold standard for diagnosis, improvements in imaging techniques in the past several years (notably transvaginal ultrasonography (TVUS) (2-D, 3-D, elastonography) and magnetic resonance imaging (MRI)) have allowed adenomyosis to be diagnosed based on imaging criteria, which has resulted in the disease being diagnosed more often in women of reproductive age (2,3). It allows adenomyosis to be diagnosed without a need for histological analysis, which has usually been achieved following a hysterectomy. Adenomyosis is considered to be a heterogeneous disease in light of the variable anatomical presentation of the lesions in the myometrium (e.g., diffusely in the myometrium or a more focal nature) and the variation in its clinical presentation. Furthermore, adenomyosis can impair the quality of life of women due to the potential disabling symptoms such as pelvic pain or abnormal uterine bleeding, and effective conservative treatments are lacking (4,5). Although the current knowledge regarding the pathogenesis of adenomyosis is only in its infancy, local (in the uterus) (6–8) and systemic imbalances (9–11) of several compounds that play key roles in immunity, cell proliferation, and oxidative stress have been described in women with adenomyosis, thus suggesting that several intertwined molecular mediators are involved. What makes understanding the pathogenesis of adenomyosis even more difficult is the heterogeneous nature of the lesions, particularly with diffuse and/or focal disease involving either the internal or the external myometrium (12–15). These distinct configurations suggest that there may be more than one mechanism to account for the pathogenesis of this disorder (11,16–18).

Metabolomics is a new discipline within the large “-omics” family of scientific disciplines, defined as the study of metabolites or low-molecular-weight products of metabolism in different entities such as cells, biological fluids, or tissues (19). It is not only used to characterize metabolic signatures that correspond to an organism’s particular state, but it also enables the identification of biomarkers (20,21). Since the metabolome corresponds to the endpoint of the omics cascade, the metabolic profile can be considered to be a snapshot of a given phenotype (22,23). Use of this approach in adenomyosis is still at a nascent stage. Indeed, few studies to date have focused on omics methods applied to adenomyosis (24), and none have examined the metabolomic signatures in women with adenomyosis, let alone according to specific adenomyosis phenotypes.

Therefore, the aim of the present study was to use a proton-nuclear magnetic resonance (^1H NMR) untargeted metabolomics approach to evaluate the serum metabolic profiles of adenomyosis versus control patients, and to determine whether different adenomyosis phenotypes have specific metabolomic signatures.

MATERIALS AND METHODS

Study Protocol and Patients

The study protocol was approved by the ethics committee of our institution (Comité Consultatif de Protection des Personnes dans la Recherche Biomédicale de Paris—Cochin, reference No. 05-2006). All of the data were fully anonymized before use.

This was a prospective cohort study that included 77 non-pregnant women of less than 42 years of age who underwent an operative laparoscopy for a benign gynecological condition at our institution. The indications for surgery were a benign gynecologic disease associated with: (i) pelvic pain defined as the presence, for at least 6 months, of dysmenorrhea and/or intermenstrual pelvic pain and/or dyspareunia of moderate to severe intensity (25); (ii) infertility defined as at least 12 months of unprotected intercourse not resulting in pregnancy (26); (iii) a pelvic mass (benign ovarian cysts, or uterine myomas for example); and (iv) others: abnormal uterine bleeding, request for tubal ligation for example. All of the women had undergone a conservative uterine surgical treatment, and no hysterectomy was performed. The included women had undergone a pelvic magnetic resonance imaging (MRI) performed by our senior radiologist, and a venous peripheral blood sample was taken during the preoperative work-up (14). Patients with cancer or borderline tumors, chronic viral infections (e.g., hepatitis and HIV), and those who did not consent to participate in the study were excluded from this population. For the purpose of this study, the women were allocated to two groups based on the MRI findings: an adenomyosis group comprising subjects with MRI findings of adenomyosis (14,27,28) and a control group of women who did not exhibit criteria for adenomyosis by MRI.

The study analysis used a prospectively managed database. For each patient, the personal history data were obtained during face-to-face interviews using a highly structured previously published questionnaire (29). The following data were recorded: age (years), parity, gravidity, height, weight, and the body mass index (BMI). To be considered as free of exogenous hormones, the participants were required to report spontaneous menses in the absence of gonadal steroid treatment in the three months prior to surgery. We also recorded current use of hormonal treatments (including progestogens, estrogen and progestogen (or progestin) - containing compounds, or gonadotropin releasing agonists (GnRH) agonists) and prior endometriosis and/or uterine surgery.

MRI examination

All of the pelvic MRI examinations were performed using a 1.5T MRI machine (Sonata, Siemens; Erlangen, Germany). The MRI data were interpreted by a senior radiologist (CB) with extensive expertise in gynecological MRI (ten years of referral practice and a mean of 1,000 scans/year). As previously described, three criteria were assessed on T₂-weighted acquisitions (27) (i) the maximal junctional zone (JZ max) thickness corresponding to a low signal intensity band of myometrium lining the endometrium (28); (ii) the JZ max to myometrial thickness ratio (ratio max) using the maximal thickness of the JZ and the corresponding thickness of the myometrium obtained at the same level of measurement; and (iii) the presence of high-intensity spots within the myometrium. In this study, diffuse adenomyosis was defined by the association of the following two criteria: (1) a JZ max of at least 12 mm and (2) a ratio max > 40 %, as previously described (14), which correspond to diffuse adenomyosis. By definition, for the purpose of this study, focal adenomyosis was

defined as MRI features of the disorder isolated to the outer myometrium and separated from the JZ by a zone of normal-appearing muscular tissue (13,30).

The women included in the control group had no evidence of adenomyosis on MRI. In the adenomyosis group, we included women with either only diffuse adenomyosis or only focal adenomyosis of the outer myometrium (FAOM) (14). Therefore, other adenomyosis phenotypes such as diffuse adenomyosis of the outer myometrium or focal adenomyosis of the inner myometrium were excluded and women with associated focal and diffuse forms were voluntarily not included in order to better characterize the metabolic profile of each of the studied adenomyosis phenotypes.

Collection of serum samples

Serum samples were collected from all of the participants in the month prior to the surgery. Briefly, samples of 5–10 ml of venous blood were collected using a peripheral venous catheter (PVC) and then centrifuged at 800xg for 12 min at 4 °C. The serum supernatants were collected, aliquoted, and stored at -70 °C within two hours of being collected until further use. NMR samples were prepared by taking 300 µL from each serum sample supernatant, after thawing on ice, followed by the addition of 300 µL of a solution containing a phosphate buffer with D₂O to obtain a final buffer concentration of 38 mM with a pH value of 7.4 that contained 2.3 mM NaN₃ as well as 2.3 mM sodium trimethylsilylpropionate-d₄ (TSP-d₄) as the NMR chemical shift reference. A total of 600 µL was then transferred into 5-mm NMR tubes for the metabolomic analysis. D₂O (12% (v/v)) was used for the field-frequency lock and shimming on the NMR spectrometer.

NMR spectroscopy and spectral processing

The NMR data were recorded on a 500.45 MHz Bruker AVANCE II spectrometer equipped

with a 5-mm $^{13}\text{C}/^1\text{H}$ cryoprobe, using a SampleXpressTM automation sample changer. ^1H spectra were obtained for each sample using a Carr-Purcell-Meiboom-Gill (CPMG) pulse sequence (31) to remove broad peaks originating from macromolecules. For each experiment, a total of 512 scans with 32,768 points were recorded using a recycle delay of 2 s and a chemical shift spectral window of 20.65 ppm, thereby resulting in a total experimental time of 33 min. The other relevant parameters were as follows: a CPMG spin-echo train of 64 ms with a spin-echo delay of 400 μs , and an acquisition time of 1.6 s. Processing of the NMR spectra was carried out using NMRProcFlow software (32). The spectra were zero-filled to 65,536 points and processed with an exponential apodization function using a line broadening of 0.3 Hz prior to Fourier transformation. They were then phased, baseline corrected, and finally referenced to the alanine methyl group signal at 1.47 ppm, which offers a better reference than TSP, for which the signal frequency varies in the presence of proteins. Individual metabolites were assigned using Chenomx NMR suite 7.1 software (Chenomx Inc. Edmonton, Canada), the human metabolome database (HMDB) (33), as well as previously published data (Dutta *et al.* 2012; Vicente-Munoz *et al.* 2016).

The spectral data were further reduced by dividing each spectrum into unevenly spaced buckets using the variable-size bucketing (VSB) method as implemented in NMRProcFlow (32) to avoid peaks lying in different consecutive integration regions. The spectral regions corresponding to TSP (ppm), water (ppm), as well as to the baseline noise (ppm), were excluded from the analysis. A total number of 121 buckets were obtained and further integrated to build the matrix of variables used in the statistical analysis.

Prior to the statistical analysis, the matrix of bucket integral values was normalized using a Quantile Normalization (QN) (36) to account for the difference in sample concentrations,

and then finally scaled to unit variance to assign the same weight to each variable, using MetaboAnalyst (37,38).

Statistical analysis

The continuous data are presented as means with the standard deviation; the categorical data as numbers and percentages. For comparison of the patients' general characteristics, we used a Pearson X^2 test or Fisher's exact probability test for the qualitative variables and the Student's t -test for the quantitative variables. Both univariate and multivariate statistical approaches were used to identify the metabolites involved in adenomyosis. Univariate analysis was carried out using the Student's t -test for comparisons between two groups, and one-way ANOVA for comparisons of more than two groups, as implemented in MetaboAnalyst (37,38). Multivariate analysis was performed using SIMCA software (Sartorius Stedim Biotech, Göttingen, Germany). A supervised orthogonal partial least-squares discriminant analysis (OPLS-DA) (39) was carried out, taking into account the class of the different samples in order to maximize class discrimination. The quality of the models that were thereby obtained was assessed with the quality factors provided by the SIMCA software, i.e., the cumulative explained variance of the observed data X , R^2X ; the cumulative explained variance of assignment Y , R^2Y ; and the estimate of the predictive ability, Q^2 . The performance of the models was further tested using CV-ANOVA (40) with a p -value < 0.05 being considered statistically significant. The main variables responsible for the class discrimination in the OPLS-DA models were identified with their Variable Importance on Projection (VIP) values. The latter corresponding to the weights of each variable in the separation.

RESULTS

Study Population

A total of 77 patients were included in this study, 32 with adenomyosis and 45 with no evidence of adenomyosis based on MRI imaging. The patient characteristics are presented in Table 1. The indications for surgery in the control group and the adenomyosis group are shown in Supplemental Table 1. No significant differences were found in terms of age, BMI, gravidity, and parity between the study group and the control group. Neither the percentage of patients undergoing hormonal treatment at the time of the surgery nor the menstrual cycle phases for the patients without hormonal treatment differed significantly between the two study groups. In the adenomyosis group, the phenotypes were distributed as follows (Supplemental Table 2): focal adenomyosis of the outer myometrium was present in 18 patients (56.2 %) and diffuse adenomyosis in 14 patients (43.8 %). The adenomyosis characteristics according to the MRI criteria used to define focal and diffuse forms of adenomyosis are detailed in Supplemental Table 2.

Serum metabolic profiles of the patients with adenomyosis compared with the controls

The first step was to obtain an overall profile for the sera of patients with features of adenomyosis. Therefore, an untargeted approach was used whereby no assumption was made about the metabolites or the metabolic pathways affected by the disease. All of the metabolites that could be detected and identified in the serum sample spectra were taken into account and investigated in terms of their relevance in the adenomyosis signature. We were able to identify a total of 97 variables, corresponding to approximately 43 metabolites (mainly to amino acids, sugars, lipids, carboxylic acids, ketoacids and derivatives). After univariate analysis, a total of 10 variables with a p -value < 0.1 (of which 9 variables had p -

values < 0.05) were identified as being relevant for the discrimination. Corresponding metabolites that were present at different levels in the adenomyosis and the control group are summarized in Figure 1a and Supplemental Figure 1. The concentrations of several metabolites, such as 3-hydroxybutyrate ($p=0.02$), glutamate ($p=0.02$), and serine ($p=0.04$), were lower in the patients with features of adenomyosis compared to the control patients. Conversely, the concentrations of proline ($p=0.01$), choline ($p=0.02$), citrate ($p=0.05$), 2-hydroxybutyrate ($p=0.04$), and creatinine ($p < 0.01$) were higher in the adenomyosis group. The OPLS-DA model was formulated to highlight the changes in metabolite levels that allowed the groups to be distinguished. The supervised OPLS-DA score plot is presented in Figure 1b/c, and it reveals a clear separation between the adenomyosis and the control groups, with relatively good model quality factors ($R^2X=0.20$, $R^2Y=0.76$, $Q^2=0.193$). The model was validated with a p -value of 0.017 obtained after a CV-ANOVA analysis (40). The main variables contributing to the separation between the two groups in the OPLS-DA model (Figure 1b) were identified and plotted as a VIP score plot (Figure 1c). Assignment of these variables revealed the same metabolites as those obtained with the univariate analysis, thereby underscoring their relevance to the pathology.

Serum metabolic profiles according to the adenomyosis phenotypes

To gain further insights regarding the metabolic changes in adenomyosis, we analyzed the serum metabolic profiles of two specific adenomyosis phenotypes (diffuse adenomyosis and FAOM) compared to controls. The results of the analysis comparing the serum metabolic profiles of the control women versus the diffuse and the FAOM forms of adenomyosis are shown in Figure 2. A significant increase in proline ($p=0.04$) and creatinine ($p < 0.01$) was observed in the FAOM and the diffuse adenomyosis groups compared to the control group.

Significantly lower levels of glutamate ($p=0.02$), 3-hydroxybutyrate ($p=0.01$), and serine ($p=0.03$), as well as an increased level of choline ($p=0.01$), were observed in the FAOM group compared to the control group. In the diffuse adenomyosis group, significantly increased levels of valine ($p = 0.04$), citrate ($p < 0.01$), and 2-hydroxybutyrate ($p < 0.01$) were observed compared to the control group. A number of significant differences in metabolite levels were also observed between diffuse and FAOM adenomyosis, including glutamate ($p < 0.01$), 3-hydroxybutyrate ($p = 0.03$), valine ($p=0.03$), and citrate ($p=0.04$), which were present at significantly higher levels in the diffuse group compared to the FAOM group. Conversely, myo-inositol ($p = 0.02$) and choline ($p=0.02$) were present at significantly lower levels in the diffuse group compared to the FAOM group.

DISCUSSION

Our study underlines the potential of using ¹H-NMR-metabolomic profiling of serum samples to identify metabolic changes associated with adenomyosis. This approach can also be used to determine the metabolic signature of different adenomyosis phenotypes. We first of all observed that women with adenomyosis have a specific serum metabolite profile, with some metabolites being present at significantly lower concentrations in the serum of patients with features of adenomyosis (e.g., 3-hydroxybutyrate, glutamate, and serine), while higher levels were observed for a number of other metabolites (e.g., proline, choline, citrate, 2-hydroxybutyrate, and creatinine) compared to the controls. Moreover, although the proline and creatinine levels were significantly higher for both of the studied phenotypes compared to the controls, we found that other metabolites in the adenomyosis serum samples exhibited different levels according to the disease phenotype. FAOM was associated with lower levels of glutamate, 3-hydroxybutyrate, and serine and an increase in the levels of choline and myo-inositol, whereas the metabolite profiles for women with only diffuse adenomyosis revealed increased levels of valine, citrate, and 2-hydroxybutyrate.

The main strengths of this study lie in the novelty of the subject and the methodological design: (i) To the best of our knowledge this is the first report on serum metabolite profiles of women with adenomyosis; (ii) Given the wide heterogeneity of adenomyosis, a novel aspect of our study is the fact that we considered the metabolomic profile in women with adenomyosis according to the phenotype of the lesions (diffuse or focal lesions of the outer myometrium) diagnosed by MRI; (iii) All of the women had undergone a pelvic MRI that was performed by a senior radiologist (CB) with expertise in gynecologic imaging, using strict previously published MRI criteria to diagnose adenomyosis (14,15); (iv) We analyzed the

metabolomic signature in the sera of women with adenomyosis. Since a key feature of serum is its high level of availability and its abundance of metabolites, its use in metabolomics studies can help with obtaining information regarding a change in metabolism associated with a given disease, without a need to resort to invasive interventions.

Our findings may nonetheless be subject to several biases: (i) This study was performed with patients who required a surgical intervention for symptomatic benign gynecological conditions. This could conceivably result in altered metabolic patterns (41). However, the women in both of the groups underwent a surgical intervention, with similar indications for surgery (Supplemental Table 1); (ii) The population studied was selected from a referral center for adenomyosis and endometriosis. This could explain the high rate of patients exhibiting an associated endometriosis. The current literature clearly indicates that adenomyosis frequently coexists with endometriosis (14,18,42–45). However, although both diseases share common features, detailed knowledge of their pathogenic pathways has revealed possible key differences (46–48). In addition, the proportion of endometriosis-affected women was comparable between the group of women with and the group without adenomyosis. Despite the high rate of endometriosis-affected women in the whole population (for both the adenomyosis and the control group), we were nonetheless able to identify metabolic alterations in serum samples in adenomyosis compared to non-affected counterparts as well as for both of the two phenotypes studied. Moreover, the metabolic pathways potentially affected by endometriosis in our previous metabolomic study in sera were not the same as those presented here (49). (iii) Another limitation stems from the absence of a consensual classification of adenomyosis: indeed, numerous types of adenomyosis have been reported, leading to several adenomyosis classifications (12,14,49,50). In our study, the results were analyzed based on MRI criteria demonstrating

evidence of diffuse adenomyosis in the inner myometrium or focal findings in the outer myometrium (14). This choice allowed for better identification of the features of each of these two types of adenomyosis lesions. We cannot exclude the possibility that the study of other MRI-defined adenomyosis phenotypes could have altered our results, notably the focal adenomyosis of the inner myometrium and the diffuse adenomyosis of the outer myometrium lesions (50); (iv) We cannot exclude that other factors could have influenced the serum metabolic profiles in our population, notably the use of hormonal treatments, or the stage of the menstrual cycle (51–53). However, no significant differences were found between the two groups in terms of the proportion of patients using hormonal treatment or according to the phase of the menstrual cycle. Moreover, no cluster according to the menstrual cycle phase or the presence of hormonal treatment was found in our analysis. Indeed, no validated model according to any of these two parameters could be obtained, even using a supervised method, as confirmed by an associated *p-value* of 1, and negative Q^2 values ($Q^2 = - 0.07$ and $Q^2 = - 0.16$, respectively), characteristic of uninformative models. (v) Finally, although our findings indicate that there are metabolomic specificities in women with features of adenomyosis, to this day, it is currently not possible to know whether these are altered due to the presence of adenomyosis and/or are responsible for the development of this pathology. At this stage, we can only present hypotheses in this regard. Additionally, in this study, we focused on serum metabolic profiles. In future studies, it would be interesting to also evaluate metabolic changes in the endometrium, given that a number of recent studies have reported changes in endometrial molecular expression profiles in women with features of adenomyosis (46,54,55).

Although adenomyosis has been studied extensively, very little is known about how metabolic pathways are affected in this disease. Various hypotheses have been put forward to explain the pathogenesis of adenomyosis (48,56,57). In the present study, we were interested in the changes in the serum metabolome of patients with features of adenomyosis, and we examined all metabolites simultaneously, with no prior knowledge of those that could potentially be affected, in order gain insights regarding the mechanisms involved in the genesis and the development of adenomyosis.

According to the only study published to date, which focused on a single metabolite related to adenomyosis in a non-human model (58), a difference in the level of citrate, both in adenomyosis uterine tissue and fluid, was observed compared with controls. Our results provide support for the notion that adenomyosis and controls can be differentiated based on citrate levels, with increased citrate levels in adenomyosis serum samples. Citrate is one of the key intermediates in the tricarboxylic acid (TCA) cycle (Figure 3). Its accumulation could arise from a potential alteration of mitochondrial function, and it could be linked to inflammatory processes (59,60), which are two phenomena that are known to be associated with adenomyosis (61–65). Other mediators of inflammation have been described in adenomyosis, notably an increase in oxidative stress (6,66). In our study, the modifications of relevant metabolites (the increased levels of 2-hydroxybutyrate and choline and the decreased levels of glutamate and serine) could reflect this imbalance between the production of reactive oxygen species (ROS) and antioxidant defenses in the adenomyosis group compared to the control group (Figure 3). Indeed, the increased levels of 2-hydroxybutyrate, choline, and creatinine in the serum samples taken from women with features of adenomyosis could reflect enhanced glutathione (GSH) synthesis, which requires glutamate and serine (among others), both of which had consistently lower levels in our

study. The GSH synthesis pathway is recognized as being important in many pathological conditions (67), and its upregulation has been shown to occur as a response to oxidative stress (68–71). In addition, GSH synthesis is also known to promote cell proliferation (67,70,72–74), which is a phenomenon that has also been described in the development of adenomyosis (75–78). Finally, several transcription factors involved in the GSH activation pathway (67,79,80) are over-expressed in adenomyosis (81–83).

Our study also revealed an increase in proline levels in the serum samples taken from women with features of adenomyosis. Proline is a very unique amino acid as it is the only proteogenic secondary amino acid. Its metabolism is hence expected to be associated with very specific pathophysiological processes. A key feature of proline is its ready availability under nutrient stress conditions due to the breakdown of collagen in the extracellular matrix (ECM) (Figure 3) (84,85). The increase in proline levels observed in the serum samples taken from women with features of adenomyosis compared to controls is in keeping with the upregulation of matrix metalloproteinases MMPs that has been observed in many diseases associated with inflammation (86), including adenomyosis, for which increased expression of MMP2 and MMP9 has been described (47,87,88). Interestingly, MMPs are known to be upregulated by estradiol (89). Impaired steroid biosynthesis has been described in adenomyosis, with an increase in the local level of estradiol (90). It is, therefore, reasonable to presume that these enzymes have a potential role in the progression and invasion of endometrial tissue in the myometrium during the development of adenomyosis. Moreover, MMPs also play a critical role in the activation of the epithelial to mesenchymal transition (EMT) (91,92). The EMT, which consists of a switch of epithelial cells to a mesenchymal profile with migratory and invasive properties, has been shown to be involved in the pathogenesis of adenomyosis (93–97). The increase in proline levels observed in the

adenomyosis serum samples could hence be a reflection of a pathogenic development driven by an EMT mechanism. Glutamine catabolism is another putative source of proline synthesis (Figure 3). Glutamine can be catabolized into glutamate by glutaminase (GLS), which can result in further production of proline. The upregulation of this pathway could contribute to the decrease in the glutamate levels observed in the adenomyosis serum samples accompanied by an increase in the levels of proline. The well-known oncogenic transcription factor c-myc (MYC), which plays a central role in the proliferation and differentiation of various types of cells (98–101), is known to markedly upregulate enzymes involved in the synthesis of proline from glutamine, while downregulating those involved in proline catabolism (100). Although no data about MYC expression in adenomyosis have been described to date, numerous studies have shown its estrogen-dependent over-expression in endometriosis (102–106). Since adenomyosis is also associated with high estrogens levels, MYC might also be upregulated in adenomyosis, thereby resulting in an increase in glutamine metabolism-mediated synthesis of proline.

However, adenomyosis is a heterogeneous disease with various clinical presentations and different anatomical forms (14,16,107). Our results revealed a number of differences in the metabolic signature according to the adenomyosis phenotype, thus supporting the notion that the pathogenesis may vary according to the location of the lesions (i.e., diffuse inner versus focal outer myometrial lesions) (14,17,18). Indeed, the level of valine was significantly increased in diffuse inner adenomyosis compared to controls and FAOM. Valine is an essential amino acid as it is a precursor of the TCA intermediate succinyl-CoA. Its increased level together with citrate accumulation thus supports the hypothesis of a defective TCA cycle, consistent with the transcriptome analysis of Herndon and coworkers that revealed a degree of mitochondrial dysfunction in diffuse adenomyosis (64). The inflammatory process

in this adenomyosis phenotype could also be related to this pathway (Figure 3) (59,60). On the other hand, FAOM appears to be characterized by a higher proliferative capacity, with a pronounced increase in choline and creatinine levels. Choline is an important component in the formation of cell membranes, and its higher level in FAOM may also be associated with increased cell turnover and proliferation (108). Interestingly, a decrease in 3-hydroxybutyrate has also been observed in FAOM. The variation of this metabolite level is consistent with the fibrotic nature of adenomyosis (109). Indeed, while the mechanism of fibrogenesis is thought to involve various molecular pathways, some studies have pointed out the presence of downregulation of fatty acid oxidation (110–113), which could explain the lower level of 3-hydroxybutyrate observed in FAOM in particular, as this metabolite is one of the endpoints of the fatty acids oxidation pathway. Changes in myo-inositol also appear to be specific to FAOM, as significantly higher levels were observed compared to controls and the diffuse group. Myo-inositol is a polyol belonging to the inositol family. Although the metabolic pathway associated with its synthesis and degradation is rather complex, this metabolite is known to play a role in various pathways such as lipid synthesis, signaling, and proliferation (Henry *et al.*, 2014; Bizzarri *et al.*, 2016; Chhetri, 2019). Altered myo-inositol levels have been shown to occur in ovarian cancer cells (114) as well as in endometriosis, where its level has been shown to correlate with the stage of the disease and with the proliferative activity of the endometriotic lesions (115). This result is in keeping with the hypothesis of a close relationship of focal lesions of the outer myometrium with severe deep infiltrating endometriosis (17,18). All up, we can assume that, although the two adenomyosis locations do have a number of features in common, they differ in several ways. The identification of specific metabolites associated with each phenotype adds considerably to the knowledge of the physiological differences at a molecular level.

Finally, a preliminary additional analysis (data not shown) was performed in order to study the relationship between metabolite levels and adenomyosis-associated symptoms (i.e., pain symptoms (dysmenorrhea, dyspareunia, and non-cyclic pelvic pain) and the presence of abnormal uterine bleeding), but no correlation between metabolite levels and adenomyosis symptoms were found. Further studies are required in this regard.

In conclusion, we here report the first untargeted serum metabolomic study of adenomyosis in humans. The use of ^1H -NMR metabolomics as an overall approach, as employed here, allowed for the identification of biomarkers associated with adenomyosis, and it highlighted specific metabolic changes associated with each of the studied phenotypes. In the context of limited information about the molecular features related to different adenomyosis phenotypes, our observations could pave the way to further research aimed at obtaining greater insights into the pathogenesis of the disease and the development of its various forms.

AUTHORS' ROLES

PS, CC, MB, and GB conceived and designed the study. MB, FK, CC, LM, CB, CM, KP, and PS contributed to the data collection. All of the authors analyzed and interpreted the data. FK, MB, GB, and PS supervised and reviewed the statistical analysis. FK, MB, PS, GB, and CC authored the manuscript. All of the authors read and approved the final version of the manuscript.

ACKNOWLEDGMENTS

The authors thank the staff members of our department for their expert assistance with the data collection. We thank MetaboParis-Santé (convention N° EX023598), an action supported by the Île-de-France Region, Université de Paris, CNRS and INSERM, for providing access to the NMR equipment.

FUNDING/CONFLICT OF INTEREST:

This study was partially supported by a Merck Biopharma France Research Grant to CC and PS. The funder had no role in the study design, the data collection and analysis, the decision to publish, and preparation of the manuscript. No additional external funding was received for this study.

REFERENCES

1. Bird CC, McElin TW, Manalo-Estrella P. The elusive adenomyosis of the uterus--revisited. *Am J Obstet Gynecol* 1972;112:583–93.
2. Chapron C, Vannuccini S, Santulli P, Abrão MS, Carmona F, Fraser IS, et al. Diagnosing adenomyosis: an integrated clinical and imaging approach. *Hum Reprod Update* 2020;
3. Liu X, Ding D, Ren Y, Guo S-W. Transvaginal Elastasonography as an Imaging Technique for Diagnosing Adenomyosis. *Reprod Sci Thousand Oaks Calif* 2018;25:498–514.
4. Ozdegirmenci O., Kayikcioglu F., Akgul M.A., Kaplan M., Karcaaltincaba M., Haberal A., et al. Comparison of levonorgestrel intrauterine system versus hysterectomy on efficacy and quality of life in patients with adenomyosis. *Fertil Steril* 2011;95:497–502.
5. Streuli I., Dubuisson J., Santulli P., De Ziegler D., Batteux F., Chapron C. An update on the pharmacological management of adenomyosis. *Expert Opin Pharmacother* 2014;15:2347–60.
6. Ota H., Igarashi S., Hatazawa J., Tanaka T. Endothelial nitric oxide synthase in the endometrium during the menstrual cycle in patients with endometriosis and adenomyosis. *Fertil Steril* 1998;69:303–8.
7. Tremellen K.P., Russell P. The distribution of immune cells and macrophages in the endometrium of women with recurrent reproductive failure. II: Adenomyosis and macrophages. *J Reprod Immunol* 2012;93:58–63.
8. Harmsen MJ, Wong CFC, Mijatovic V, Griffioen AW, Groenman F, Hehenkamp WJK, et al. Role of angiogenesis in adenomyosis-associated abnormal uterine bleeding and subfertility: a systematic review. *Hum Reprod Update* 2019;25:646–70.
9. Xiaoyu L, Weiyuan Z, Ping J, Anxia W, Liane Z. Comparative serum proteomic analysis of adenomyosis using the isobaric tags for relative and absolute quantitation technique. *Fertil Steril* 2013;100:505–10.
10. Fan Y, Liu Y, Chen H, Chen W, Wang L. Serum level concentrations of pro-inflammatory cytokines in patients with adenomyosis. *Biomed. Res.* 2017;
11. Bourdon M, Santulli P, Chouzenoux S, Maignien C, Bailly K, Andrieu M, et al. The Disease Phenotype of Adenomyosis-Affected Women Correlates With Specific Serum Cytokine Profiles. *Reprod Sci Thousand Oaks Calif* 2018;1933719118816852.
12. Gordts S, Brosens JJ, Fusi L, Benagiano G, Brosens I. Uterine adenomyosis: a need for uniform terminology and consensus classification. *Reprod Biomed Online* 2008;17:244–8.
13. Kishi Y, Suginami H, Kuramori R, Yabuta M, Suginami R, Taniguchi F. Four subtypes of adenomyosis assessed by magnetic resonance imaging and their specification. *Am J Obstet Gynecol* 2012;207:114.e1-7.
14. Chapron C, Tosti C, Marcellin L, Bourdon M, Lafay-Pillet M-C, Millischer A-E, et al. Relationship between the magnetic resonance imaging appearance of adenomyosis and endometriosis phenotypes. *Hum Reprod Oxf Engl* 2017;32:1393–401.
15. Bazot M, Daraï E. Role of transvaginal sonography and magnetic resonance imaging in the diagnosis of uterine adenomyosis. *Fertil Steril* 2018;109:389–97.
16. Kishi Y, Shimada K, Fujii T, Uchiyama T, Yoshimoto C, Konishi N, et al. Phenotypic characterization of adenomyosis occurring at the inner and outer myometrium. *PloS One* 2017;12:e0189522.
17. Marcellin L, Santulli P, Bortolato S, Morin C, Millischer AE, Borghese B, et al. Anterior Focal Adenomyosis and Bladder Deep Infiltrating Endometriosis: Is There a Link? *J Minim Invasive Gynecol* 2018;25:896–901.
18. Khan KN, Fujishita A, Koshiba A, Kuroboshi H, Mori T, Ogi H, et al. Biological differences between intrinsic and extrinsic adenomyosis with coexisting deep infiltrating

endometriosis. *Reprod Biomed Online* 2019;39:343–53.

19. Klassen A, Faccio AT, Canuto GAB, da Cruz PLR, Ribeiro HC, Tavares MFM, et al. Metabolomics: Definitions and Significance in Systems Biology. *Adv Exp Med Biol* 2017;965:3–17.
20. Pallet N, Thervet E, Beaune P, Karras A, Bertho G. The urinary metabolome of chronic kidney disease. *Kidney Int* 2014;85:1239–40.
21. Sinclair K, Dudley E. Metabolomics and Biomarker Discovery. *Adv Exp Med Biol* 2019;1140:613–33.
22. Patti GJ, Yanes O, Siuzdak G. Metabolomics: the apogee of the omic trilogy. *Nat Rev Mol Cell Biol* 2012;13:263–9.
23. Zhang A, Sun H, Yan G, Wang P, Wang X. Metabolomics for Biomarker Discovery: Moving to the Clinic. *BioMed Res Int [Internet]* 2015 [cited 2020 Mar 27];2015. Available from: <https://www.ncbi.nlm.nih.gov/pmc/articles/PMC4452245/>
24. Yang H, Lau WB, Lau B, Xuan Y, Zhou S, Zhao L, et al. A Mass Spectrometric Insight into the Origins of Benign Gynecological Disorders. *Mass Spectrom Rev* 2017;36:450–70.
25. Fedele L, Bianchi S, Zanconato G, Bergamini V, Berlanda N, Carmignani L. Long-term follow-up after conservative surgery for bladder endometriosis. *Fertil Steril* 2005;83:1729–33.
26. Marcoux S, Maheux R, Bérubé S. Laparoscopic surgery in infertile women with minimal or mild endometriosis. Canadian Collaborative Group on Endometriosis. *N Engl J Med* 1997;337:217–22.
27. Bazot M, Cortez A, Darai E, Rouger J, Chopier J, Antoine JM, et al. Ultrasonography compared with magnetic resonance imaging for the diagnosis of adenomyosis: correlation with histopathology. *Hum Reprod Oxf Engl* 2001;16:2427–33.
28. Novellas S, Chassang M, Delotte J, Toullalan O, Chevallier A, Bouaziz J, et al. MRI characteristics of the uterine junctional zone: from normal to the diagnosis of adenomyosis. *AJR Am J Roentgenol* 2011;196:1206–13.
29. Chapron C, Souza C, de Ziegler D, Lafay-Pillet M-C, Ngô C, Bijaoui G, et al. Smoking habits of 411 women with histologically proven endometriosis and 567 unaffected women. *Fertil Steril* 2010;94:2353–5.
30. Arnold LL, Ascher SM, Schrufer JJ, Simon JA. The nonsurgical diagnosis of adenomyosis. *Obstet Gynecol* 1995;86:461–5.
31. Meiboom S, Gill D. Modified spin-echo method for measuring nuclear relaxation times. *Rev Sci Instrum* 1958;29:688–91.
32. Jacob D, Deborde C, Lefebvre M, Maucourt M, Moing A. NMRProcFlow: a graphical and interactive tool dedicated to 1D spectra processing for NMR-based metabolomics. *Metabolomics* 2017;13:36.
33. Wishart DS, Tzur D, Knox C, Eisner R, Guo AC, Young N, et al. HMDB: the Human Metabolome Database. *Nucleic Acids Res* 2007;35:D521-526.
34. Dutta M, Joshi M, Srivastava S, Lodh I, Chakravarty B, Chaudhury K. A metabolomics approach as a means for identification of potential biomarkers for early diagnosis of endometriosis. *Mol Biosyst* 2012;8:3281–7.
35. Vicente-Munoz S, Morcillo I, Puchades-Carrasco L, Paya V, Pellicer A, Pineda-Lucena A. Pathophysiologic processes have an impact on the plasma metabolomic signature of endometriosis patients. *Fertil Steril* 2016;106:1733–+.
36. Kohl SM, Klein MS, Hochrein J, Oefner PJ, Spang R, Gronwald W. State-of-the art data normalization methods improve NMR-based metabolomic analysis. *Metabolomics* 2012;8:146–60.
37. Xia J, Psychogios N, Young N, Wishart DS. MetaboAnalyst: a web server for

- metabolomic data analysis and interpretation. *Nucleic Acids Res* 2009;37:W652–60.
38. Chong J, Soufan O, Li C, Caraus I, Li S, Bourque G, et al. MetaboAnalyst 4.0: towards more transparent and integrative metabolomics analysis. *Nucleic Acids Res* 2018;46:W486–94.
 39. Trygg J, Wold S. Orthogonal projections to latent structures (O-PLS). *J Chemom* 2002;16:119–28.
 40. Eriksson L, Trygg J, Wold S. CV-ANOVA for significance testing of PLS and OPLS® models. *J Chemom* 2008;22:594–600.
 41. Yang H, Lau WB, Lau B, Xuan Y, Zhou S, Zhao L, et al. A mass spectrometric insight into the origins of benign gynecological disorders. *Mass Spectrom Rev* 2017;36:450–70.
 42. Kunz G, Beil D, Huppert P, Noe M, Kissler S, Leyendecker G. Adenomyosis in endometriosis--prevalence and impact on fertility. Evidence from magnetic resonance imaging. *Hum Reprod Oxf Engl* 2005;20:2309–16.
 43. Di Donato N, Montanari G, Benfenati A, Leonardi D, Bertoldo V, Monti G, et al. Prevalence of adenomyosis in women undergoing surgery for endometriosis. *Eur J Obstet Gynecol Reprod Biol* 2014;181:289–93.
 44. Leyendecker G, Bilgicyildirim A, Inacker M, Stalf T, Huppert P, Mall G, et al. Adenomyosis and endometriosis. Re-visiting their association and further insights into the mechanisms of auto-traumatisation. An MRI study. *Arch Gynecol Obstet* 2015;291:917–32.
 45. Eisenberg VH, Arbib N, Schiff E, Goldenberg M, Seidman DS, Soriano D. Sonographic Signs of Adenomyosis Are Prevalent in Women Undergoing Surgery for Endometriosis and May Suggest a Higher Risk of Infertility. *BioMed Res Int* 2017;2017:8967803.
 46. Benagiano G, Brosens I, Habiba M. Structural and molecular features of the endomyometrium in endometriosis and adenomyosis. *Hum Reprod Update* 2014;20:386–402.
 47. Vannuccini S, Tosti C, Carmona F, Huang SJ, Chapron C, Guo S-W, et al. Pathogenesis of adenomyosis: an update on molecular mechanisms. *Reprod Biomed Online* 2017;35:592–601.
 48. Guo S-W. The Pathogenesis of Adenomyosis vis-à-vis Endometriosis. *J Clin Med* [Internet] 2020 [cited 2020 Apr 16];9. Available from: <https://www.ncbi.nlm.nih.gov/pmc/articles/PMC7073526/>
 49. Kishi Y, Suginami H, Kuramori R, Yabuta M, Suginami R, Taniguchi F. Four subtypes of adenomyosis assessed by magnetic resonance imaging and their specification. *Am J Obstet Gynecol* 2012;207:114.e1-7.
 50. Bazot M, Daraï E. Role of transvaginal sonography and magnetic resonance imaging in the diagnosis of uterine adenomyosis. *Fertil Steril* 2018;109:389–97.
 51. Draper CF, Duisters K, Weger B, Chakrabarti A, Harms AC, Brennan L, et al. Menstrual cycle rhythmicity: metabolic patterns in healthy women. *Sci Rep* 2018;8:14568.
 52. Wallace M, Hashim YZH-Y, Wingfield M, Culliton M, McAuliffe F, Gibney MJ, et al. Effects of menstrual cycle phase on metabolomic profiles in premenopausal women. *Hum Reprod Oxf Engl* 2010;25:949–56.
 53. Ruoppolo M, Campesi I, Scolamiero E, Pecce R, Caterino M, Cherchi S, et al. Serum metabolomic profiles suggest influence of sex and oral contraceptive use. *Am J Transl Res* 2014;6:614–24.
 54. Hever A, Roth RB, Hevezi PA, Lee J, Willhite D, White EC, et al. Molecular characterization of human adenomyosis. *Mol Hum Reprod* 2006;12:737–48.
 55. Herndon CN, Aghajanova L, Balayan S, Erikson D, Barragan F, Goldfien G, et al. Global Transcriptome Abnormalities of the Eutopic Endometrium From Women With Adenomyosis. *Reprod Sci Thousand Oaks Calif* 2016;23:1289–303.

56. Bergeron C., Amant F., Ferenczy A. Pathology and physiopathology of adenomyosis. *Best Pract Res Clin Obstet Gynaecol* 2006;20:511–21.
57. Leyendecker G, Wildt L. A new concept of endometriosis and adenomyosis: tissue injury and repair (TIAR). *Horm Mol Biol Clin Investig* 2011;5:125–42.
58. Iizuka A, Nakabachi A, Mori T, Park MK, Fujii Y, Nagasawa H. Changes in citrate concentration in the mouse uterus with experimentally-induced adenomyosis. *Life Sci* 1995;58:397–403.
59. Iacobazzi V, Infantino V. Citrate--new functions for an old metabolite. *Biol Chem* 2014;395:387–99.
60. Williams NC, O'Neill LAJ. A Role for the Krebs Cycle Intermediate Citrate in Metabolic Reprogramming in Innate Immunity and Inflammation. *Front Immunol* [Internet] 2018 [cited 2020 Apr 20];9. Available from: <https://www.frontiersin.org/articles/10.3389/fimmu.2018.00141/full>
61. Ota H, Igarashi S, Hatazawa J, Tanaka T. Is adenomyosis an immune disease? *Hum Reprod Update* 1998;4:360–7.
62. Ding X, Wang L, Ren Y, Zheng W. Differences in mitochondrial proteins in the eutopic endometrium of patients with adenomyosis and endometriosis identified using surface-enhanced laser desorption/ionization time-of-flight mass spectrometry. *J Int Med Res* 2010;38:987–93.
63. Carrarelli P, Yen C-F, Funghi L, Arcuri F, Tosti C, Bifulco G, et al. Expression of Inflammatory and Neurogenic Mediators in Adenomyosis: A Pathogenetic Role. *Reprod Sci* Thousand Oaks Calif 2016;
64. Herndon CN, Aghajanova L, Balayan S, Erikson D, Barragan F, Goldfien G, et al. Global Transcriptome Abnormalities of the Eutopic Endometrium From Women With Adenomyosis: *Reprod Sci* [Internet] 2016 [cited 2020 Apr 15]; Available from: <https://journals.sagepub.com/doi/10.1177/1933719116650758>
65. Orazov MR, Radzinsky VE, Nosenko EN, Khamoshina MB, Dukhin AO, Lebedeva MG. Immune-inflammatory predictors of the pelvic pain syndrome associated with adenomyosis. *Gynecol Endocrinol* 2017;33:44–6.
66. Kamada Y, Nakatsuka M, Asagiri K, Noguchi S, Habara T, Takata M, et al. GnRH agonist-suppressed expression of nitric oxide synthases and generation of peroxynitrite in adenomyosis. *Hum Reprod* 2000;15:2512–9.
67. Lu SC. Regulation of glutathione synthesis. *Mol Aspects Med* 2009;30:42–59.
68. Landaas S, Pettersen JE. Clinical Conditions Associated with Urinary Excretion of 2-Hydroxybutyric Acid. *Scand J Clin Lab Invest* 1975;35:259–66.
69. Lord RS, Bralley JA. Clinical applications of urinary organic acids. Part I: Detoxification markers. *Altern Med Rev J Clin Ther* 2008;13:205–15.
70. Lu SC. GLUTATHIONE SYNTHESIS. *Biochim Biophys Acta* 2013;1830:3143–53.
71. Dash PK, Hergenroeder GW, Jeter CB, Choi HA, Kobori N, Moore AN. Traumatic Brain Injury Alters Methionine Metabolism: Implications for Pathophysiology. *Front Syst Neurosci* 2016;10:36.
72. Shaw JP, Chou IN. Elevation of intracellular glutathione content associated with mitogenic stimulation of quiescent fibroblasts. *J Cell Physiol* 1986;129:193–8.
73. Huang ZZ, Chen C, Zeng Z, Yang H, Oh J, Chen L, et al. Mechanism and significance of increased glutathione level in human hepatocellular carcinoma and liver regeneration. *FASEB J Off Publ Fed Am Soc Exp Biol* 2001;15:19–21.
74. Bansal A, Simon MC. Glutathione metabolism in cancer progression and treatment resistance. *J Cell Biol* 2018;217:2291–8.
75. Zou Y, Liu F-Y, Wang L-Q, Guo J-B, Yang B-C, Wan X-D, et al. Downregulation of DNA methyltransferase 3 alpha promotes cell proliferation and invasion of ectopic

endometrial stromal cells in adenomyosis. *Gene* 2017;604:41–7.

76. Li J, Yanyan M, Mu L, Chen X, Zheng W. The expression of Bcl-2 in adenomyosis and its effect on proliferation, migration, and apoptosis of endometrial stromal cells. *Pathol Res Pract* 2019;215:152477.
77. Shi B, Tu H, Sha L, Luo X, Wu W, Su Y, et al. Upregulation of long noncoding RNA TUG1 by EGR1 promotes adenomyotic epithelial cell migration and invasion through recruiting EZH2 and suppressing TIMP2. *Mol Reprod Dev* 2019;86:239–47.
78. Lin S-L, Duan H, Wang S, Li J-J. Overexpression of Lin28B Promoted the Proliferation of Adenomyotic Smooth Muscle Cells of the Junctional Zone via Regulating Let-7a. *Reprod Sci Thousand Oaks Calif* 2020;27:1156–63.
79. Meng Q, Peng Z, Chen L, Si J, Dong Z, Xia Y. Nuclear Factor- κ B Modulates Cellular Glutathione and Prevents Oxidative Stress in Cancer Cells. *Cancer Lett* 2010;299:45–53.
80. Y H, Na J, Ti T, Ve V, Sj H. Interleukin-1 β protects astrocytes against oxidant-induced injury via an NF- κ B-dependent upregulation of glutathione synthesis. *Glia* 2015;63:1568–80.
81. Li B, Chen M, Liu X, Guo S-W. Constitutive and tumor necrosis factor- α -induced activation of nuclear factor- κ B in adenomyosis and its inhibition by andrographolide. *Fertil Steril* 2013;100:568–77.
82. Park H, Kim S-H, Cho YM, Ihm HJ, Oh YS, Hong SH, et al. Increased expression of nuclear factor kappa-B p65 subunit in adenomyosis. *Obstet Gynecol Sci* 2016;59:123–9.
83. Chen N, Du B, Zhou H, Shen F, Li J, Xie Z. Abnormal expression of Nrf2 may play an important role in the pathogenesis and development of adenomyosis. *PLoS ONE [Internet]* 2017 [cited 2020 Apr 24];12. Available from: <https://www.ncbi.nlm.nih.gov/pmc/articles/PMC5560740/>
84. Phang JM, Pandhare J, Liu Y. The Metabolism of Proline as Microenvironmental Stress Substrate. *J Nutr* 2008;138:2008S-2015S.
85. Pandhare J, Cooper SK, Donald SP, Phang JM. Regulation and Function of Proline Oxidase under Nutrient Stress. *J Cell Biochem* 2009;107:759–68.
86. Parks WC, Wilson CL, López-Boado YS. Matrix metalloproteinases as modulators of inflammation and innate immunity. *Nat Rev Immunol* 2004;4:617–29.
87. Li T, Li Y-G, Pu D-M. Matrix Metalloproteinase-2 and -9 Expression Correlated with Angiogenesis in Human Adenomyosis. *Gynecol Obstet Invest* 2006;62:229–35.
88. Tokyol C, Aktepe F, Dilek FH, Sahin O, Arioz DT. Expression of cyclooxygenase-2 and matrix metalloproteinase-2 in adenomyosis and endometrial polyps and its correlation with angiogenesis. *Int J Gynecol Pathol Off J Int Soc Gynecol Pathol* 2009;28:148–56.
89. Braundmeier AG, Fazleabas AT, Lessey BA, Guo H, Toole BP, Nowak RA. Extracellular Matrix Metalloproteinase Inducer Regulates Metalloproteinases in Human Uterine Endometrium. *J Clin Endocrinol Metab* 2006;91:2358–65.
90. Mehaseb MK, Panchal R, Taylor AH, Brown L, Bell SC, Habiba M. Estrogen and progesterone receptor isoform distribution through the menstrual cycle in uteri with and without adenomyosis. *Fertil Steril* 2011;95:2228–35, 2235.e1.
91. Radisky ES, Radisky DC. Matrix metalloproteinase-induced epithelial-mesenchymal transition in breast cancer. *J Mammary Gland Biol Neoplasia* 2010;15:201–12.
92. Scheau C, Badarau IA, Costache R, Caruntu C, Mihai GL, Didilescu AC, et al. The Role of Matrix Metalloproteinases in the Epithelial-Mesenchymal Transition of Hepatocellular Carcinoma [Internet]. *Anal. Cell. Pathol.* 2019 [cited 2020 Apr 17];2019:e9423907. Available from: <https://www.hindawi.com/journals/acp/2019/9423907/>
93. Oh SJ, Shin J-H, Kim TH, Lee HS, Yoo J-Y, Ahn JY, et al. β -Catenin activation contributes to the pathogenesis of adenomyosis through epithelial–mesenchymal transition. *J Pathol* 2013;231:210–22.

94. Huang B-S, Tsai H-W, Wang P-H, Twu N-F, Yen M-S, Chen Y-J. Epithelial-to-mesenchymal transition in the development of adenomyosis. *Gynecol Minim Invasive Ther* 2015;4:55–60.
95. García-Solares J, Donnez J, Donnez O, Dolmans M-M. Pathogenesis of uterine adenomyosis: invagination or metaplasia? *Fertil Steril* 2018;109:371–9.
96. Khan KN. Role of Epithelial-Mesenchymal Transition in Human Adenomyosis: A New Insight into Its Pathogenesis [Internet]. In: Sugino N, editor. *Uterine Fibroids and Adenomyosis*. Singapore: Springer; 2018 [cited 2020 Apr 16]. p. 129–40. Available from: https://doi.org/10.1007/978-981-10-7167-6_9
97. Zheng D, Duan H, Wang S, Xu Q, Gan L, Li J, et al. FAK regulates epithelial-mesenchymal transition in adenomyosis. *Mol Med Rep* 2018;18:5461–72.
98. Gao P, Tchernyshyov I, Chang T-C, Lee Y-S, Kita K, Ochi T, et al. c-Myc suppression of miR-23a/b enhances mitochondrial glutaminase expression and glutamine metabolism. *Nature* 2009;458:762–5.
99. Wise DR, Thompson CB. Glutamine addiction: a new therapeutic target in cancer. *Trends Biochem Sci* 2010;35:427–33.
100. Liu W, Le A, Hancock C, Lane AN, Dang CV, Fan TW-M, et al. Reprogramming of proline and glutamine metabolism contributes to the proliferative and metabolic responses regulated by oncogenic transcription factor c-MYC. *Proc Natl Acad Sci U S A* 2012;109:8983–8.
101. Liu L, Zhang J, Yang X, Fang C, Xu H, Xi X. SALL4 as an Epithelial-Mesenchymal Transition and Drug Resistance Inducer through the Regulation of c-Myc in Endometrial Cancer. *PloS One* 2015;10:e0138515.
102. Dubik D, Shiu RP. Mechanism of estrogen activation of c-myc oncogene expression. *Oncogene* 1992;7:1587–94.
103. Fujimoto J, Hori M, Ichigo S, Nishigaki M, Tamaya T. Tissue differences in the expression of mRNAs of Ha-ras, c-myc, fos and jun in human uterine endometrium, myometrium and leiomyoma under the influence of estrogen/progesterone. *Tumour Biol J Int Soc Oncodevelopmental Biol Med* 1994;15:311–7.
104. Bircan S, Ensari A, Ozturk S, Erdogan N, Dundar I, Ortac F. Immunohistochemical analysis of c-myc, c-jun and estrogen receptor in normal, hyperplastic and neoplastic endometrium. *Pathol Oncol Res POR* 2005;11:32–9.
105. Pellegrini C, Gori I, Achtari C, Hornung D, Chardonnens E, Wunder D, et al. The expression of estrogen receptors as well as GREB1, c-MYC, and cyclin D1, estrogen-regulated genes implicated in proliferation, is increased in peritoneal endometriosis. *Fertil Steril* 2012;98:1200–8.
106. Proestling K, Birner P, Gamperl S, Nirtl N, Marton E, Yerlikaya G, et al. Enhanced epithelial to mesenchymal transition (EMT) and upregulated MYC in ectopic lesions contribute independently to endometriosis. *Reprod Biol Endocrinol RBE [Internet]* 2015 [cited 2020 Apr 17];13. Available from: <https://www.ncbi.nlm.nih.gov/pmc/articles/PMC4511248/>
107. Exacoustos C, Lauriola I, Lazzeri L, De Felice G, Zupi E. Complications during pregnancy and delivery in women with untreated rectovaginal deep infiltrating endometriosis. *Fertil Steril* 2016;106:1129-1135.e1.
108. Ahmed KA, Chinnaiyan P. Applying Metabolomics to Understand the Aggressive Phenotype and Identify Novel Therapeutic Targets in Glioblastoma. *Metabolites* 2014;4:740–50.
109. Vannuccini S., Tosti C., Carmona F., Huang S.J., Chapron C., Guo S.-W., et al. Pathogenesis of adenomyosis: an update on molecular mechanisms. *Reprod Biomed Online* 2017;35:592–601.

110. Watanabe K, Fujii H, Takahashi T, Kodama M, Aizawa Y, Ohta Y, et al. Constitutive Regulation of Cardiac Fatty Acid Metabolism through Peroxisome Proliferator-activated Receptor α Associated with Age-dependent Cardiac Toxicity. *J Biol Chem* 2000;275:22293–9.
111. Kang HM, Ahn SH, Choi P, Ko Y-A, Han SH, Chinga F, et al. Defective fatty acid oxidation in renal tubular epithelial cells plays a key role in kidney fibrosis development. *Nat Med* 2015;21:37–46.
112. Chung KW, Lee EK, Lee MK, Oh GT, Yu BP, Chung HY. Impairment of PPAR α and the Fatty Acid Oxidation Pathway Aggravates Renal Fibrosis during Aging. *J Am Soc Nephrol* 2018;1223–37.
113. Jang H-S, Noh MR, Kim J, Padanilam BJ. Defective Mitochondrial Fatty Acid Oxidation and Lipotoxicity in Kidney Diseases. *Front Med [Internet]* 2020 [cited 2020 May 29];7. Available from: <https://www.frontiersin.org/articles/10.3389/fmed.2020.00065/full#B26>
114. Ferretti A, D’Ascenzo S, Knijn A, Iorio E, Dolo V, Pavan A, et al. Detection of polyol accumulation in a new ovarian carcinoma cell line, CABA I: a¹H NMR study. *Br J Cancer* 2002;86:1180.
115. Dutta M, Singh B, Joshi M, Das D, Subramani E, Maan M, et al. Metabolomics reveals perturbations in endometrium and serum of minimal and mild endometriosis. *Sci Rep* 2018;8:6466.

Figure captions

Figure 1. Univariate and multivariate analysis of serum samples collected from the control patients (n=45) and the patients with features of adenomyosis (n=32).

a. Variables identified as relevant in the discrimination between the control and the adenomyosis samples following univariate analysis.

[†]The statistical analysis was performed using the Student's *t*-test; * *p*-value < 0.1; ** *p*-value < 0.05; in bold: metabolites with lower concentrations in the patients with features of adenomyosis compared to the controls; in italics: metabolites with higher concentrations in the patients with adenomyosis compared to the controls.

b/c. Score plot of the supervised multivariate analysis obtained using orthogonal partial least-squares discriminant analysis (OPLS-DA) of serum samples collected from the control patients and the patients with adenomyosis. **b.** OPLS-DA score plot. The corresponding quality factors were as follows: $R^2X = 0.20$, $R^2Y = 0.76$, and $Q^2 = 0.193$. The OPLS-DA model was validated with a *p*-value of 0.017 obtained using CV-ANOVA; **c.** Variable importance in projection (VIP) score plot showing the variables contributing the most to the group discrimination in the OPLS-DA model, sorted according to their VIP scores. The X-axis indicates the center of the chemical shift range of the corresponding bucket, whereas the Y-axis corresponds to the VIP score, i.e., the weight of each variable in the group separation. Corresponding metabolites are indicated on the top of each box. Metabolites that had increased levels in patients with features of adenomyosis are indicated in black; those that had reduced levels are indicated in grey. The results from the univariate analysis using the Student's *t*-test are also indicated: * *p*-value < 0.1, and ** *p*-value < 0.05.

Figure 2. Boxplots showing the significant differences in the concentrations of metabolites between the control samples (n=45) and the adenomyosis samples according to the phenotype (diffuse adenomyosis n=14, light-grey boxes; and focal adenomyosis of the outer myometrium (FAOM) group n=18, dark-grey boxes).

The results are presented as boxplots that show the difference in the concentrations of metabolites using one-way ANOVA. Statistically significant differences between pairs of groups obtained using the Student's *t*-test are indicated by an asterisk (* p -value < 0.1, and ** p -value < 0.05).

Figure 3. Schematic representation of the putative metabolic pathways altered in adenomyosis.

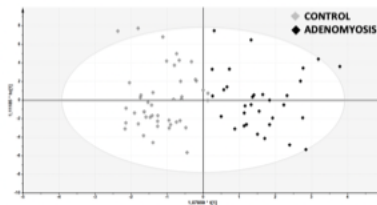
FA: fatty acids; ECM: extracellular matrix; GSH: Glutathione; MYC: oncogenic transcription factor c-Myc; OS: oxidative stress

Enzymes are indicated in red boxes, ACLY: ATP citrate lyase; CIC: Citrate carrier; GLS: Glutaminase; MMPs: Matrix metalloproteinases. The metabolic pathways that are potentially up- or down-regulated in adenomyosis are indicated in blue and red, respectively. The metabolites for which the levels were statistically different between the adenomyosis and the control samples are indicated in black, and the variation of their concentrations in adenomyosis serum samples is indicated with a grey arrow. Oxidative stress associated with adenomyosis could activate the glutathione synthesis pathway, thereby resulting in the release of 2-hydroxybutyrate, choline, and creatine, which is further converted into creatinine. The latter pathway also requires serine and glutamate, thus contributing to their lower levels in adenomyosis. A defective TCA cycle, as well as glutamine

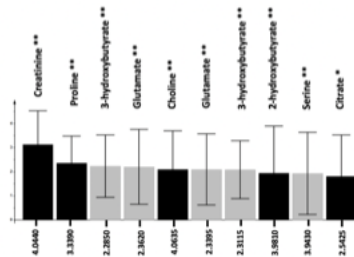
catabolism, results in the accumulation of citrate, which can be further converted in the cytoplasm to oxaloacetate, which is involved in inflammatory processes, and in acetyl-CoA, which activates the fatty acid synthesis pathway. In keeping with this, the level of 3-hydroxybutyrate, derived from fatty acids oxidation, is lower in adenomyosis. Overexpression of MMPs in adenomyosis, potentially upon estrogen activation, results in upregulation of collagen degradation in the ECM, thereby accounting for the accumulation of proline, in addition to glutamine catabolism towards proline synthesis.

BUCKET CENTER	¹ H CHEMICAL SHIFT RANGE (ppm)	METABOLITES	p-value [†]
2.2850	2.274 – 2.296	3-HYDROXYBUTYRATE **	0.016
2.3115	2.298 – 2.325	3-HYDROXYBUTYRATE **	0.024
2.3395	2.325 – 2.354	GLUTAMATE **	0.0236
2.3620	2.354 – 2.370	GLUTAMATE **	0.0170
2.5425	2.526 – 2.559	CITRATE *	0.051
3.3390	3.332 – 3.346	PROLINE **	0.010
3.9430	3.939 – 3.947	SERINE **	0.038
3.9810	3.976 – 3.986	2-HYDROXYBUTYRATE **	0.036
4.0440	4.036 – 4.052	CREATININE **	0.001
4.0635	4.053 – 4.074	CHOLINE **	0.023

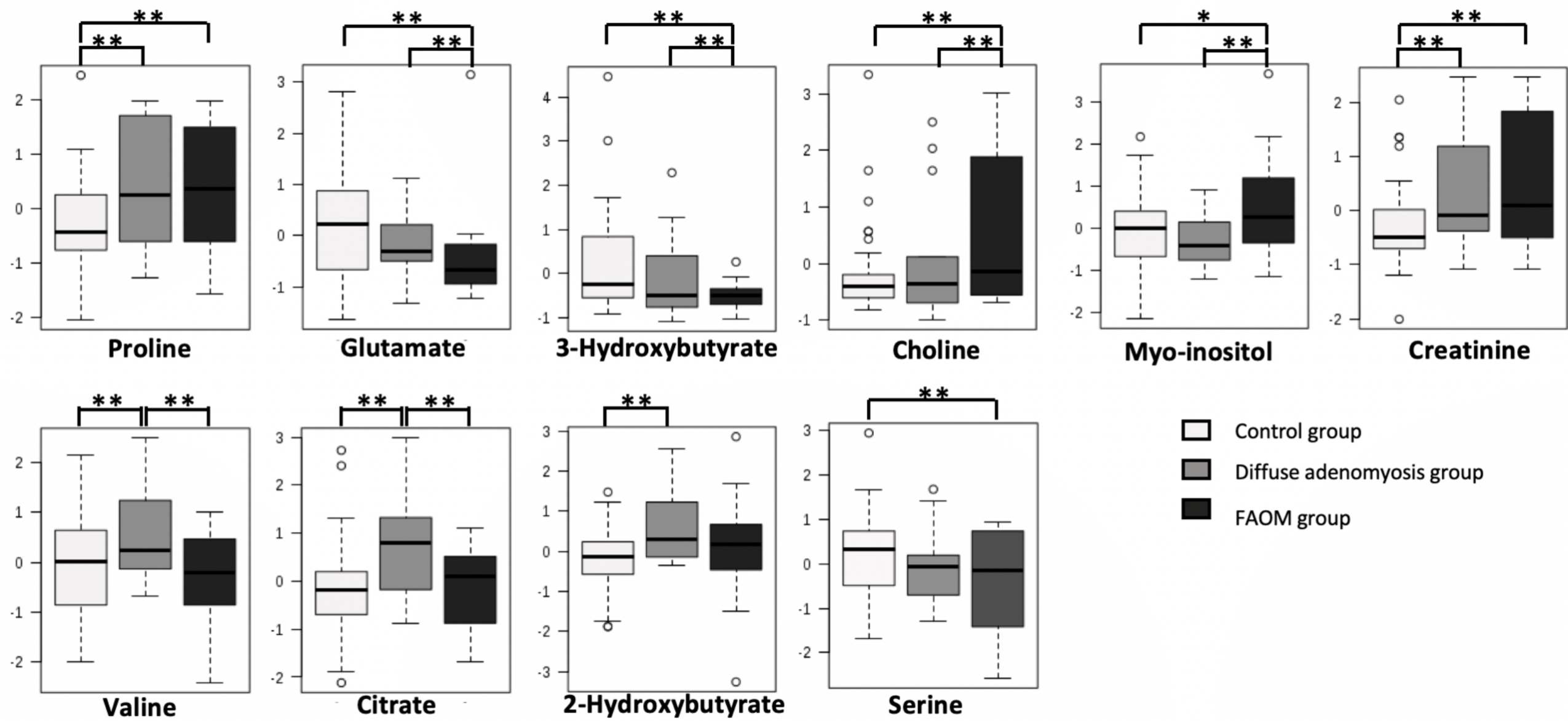
a.



b.



c.



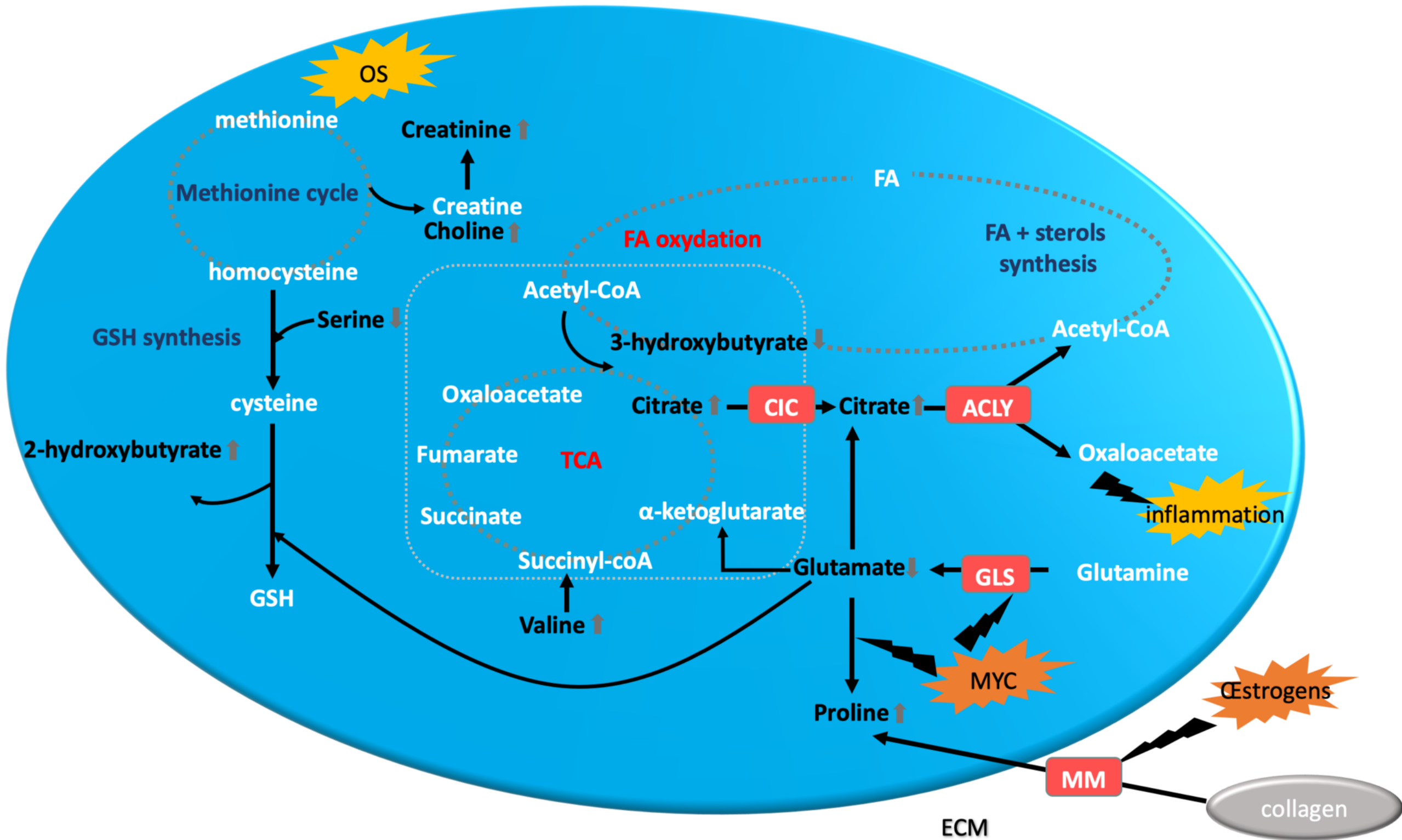


Table 1. Baseline characteristics of the patients

	ADE (-) N = 45	ADE (+) N = 32	p-value*
Patient age (years)	32.6 ± 5.1	33.8 ± 4.1	0.303
BMI (kg/m²)	22.8 ± 4.1	21.6 ± 2.6	0.131
Smoker	10 (22.2)	10 (31.3)	0.374
Gravidity	0.53 ± 0.92	0.81 ± 1.09	0.228
Parity	0.24 ± 0.57	0.53 ± 0.88	0.112
Endometriosis status			0.554
No endometriosis	10 (22.2)	9 (28.1)	
Associated endometriosis	35 (77.8)	23 (71.9)	
Hormonal treatment			0.245
No treatment	27 (60.0)	16 (50.0)	
GnRH agonist	2 (4.4)	1 (3.1)	
Progestin	14 (31.1)	9 (28.1)	
Estroprogestin pills	2 (4.4)	6 (18.8)	
Associated leiomyomas	10 (22.2)	4 (12.5)	0.276
Menstrual phase^E			0.356
Follicular phase	16 (59.3)	6 (37.5)	
Luteal phase	8 (29.6)	8 (50.0)	
Unknown	3 (11.1)	2 (12.5)	

ADE, Adenomyosis; ADE (-), women without adenomyosis; ADE (+), adenomyosis-affected women; BMI, Body mass index; GnRH, Gonadotropin-releasing hormone.

The data are means ± the standard deviation or n (%), unless specified otherwise – *Chi² test or t-test, as appropriate